Proceedings of the ASME 2018 37th International Conference on Ocean, Offshore and Arctic Engineering
OMAE2018
June 17-22, , Madrid, Spain

OMAE2018-77962

ACTIVE LOAD MITIGATION TO COUNTER THE FATIGUE DAMAGE CONTRIBUTIONS FROM UNAVAILABILITY IN OFFSHORE WIND TURBINES

Stian H. Sørum*
Emil Smilden
Jørgen Amdahl
Asgeir J. Sørensen
Centre for Autonomous Marine Operations and Systems
Department of Marine Technology
Norwegian University of Science and Technology
NO-7491 Trondheim
Norway
Email: stian.h.sorum@ntnu.no

ABSTRACT

The offshore wind industry continues to grow, but there is still a need for more economical designs. As unavailability conditions can be critical for the fatigue damage in support structures, design standards use conservative values for availability. This leads to most turbines having an unused fatigue capacity at the end of the lifetime. This paper investigates the potential for reducing this unused capacity in order to reduce the capital expenses. The proposed strategy is to design the turbines for a higher availability, closer to the expected value. For individual turbines that experience lower availability than the design value, active load mitigation is imposed to reduce the fatigue damage. The potential of this methods is explored, together with its limitations. It is found that the effect of faults occurring early in the turbines lifetime can be reduced. This is not the case for faults occurring towards the end of the lifetime.

INTRODUCTION

While there is an increasing growth in installed capacity of offshore wind turbines (OWTs) [1], the levelized cost of energy must still be reduced in order to make offshore wind harvesting economically feasible compared to other renewable energy sources. Up until present, monopile foundations have been regarded as the most economical solution for bottom-fixed turbines in shallow water depths. While simple to construct, these foundations are subject to larger hydrodynamic loads than alternative designs, such as jacket support structures. Despite this, monopile foundations are dominating new projects, where both increased turbine sizes and water depths [1] lead to further increased hydrodynamic loading.

Several possible approaches are available for reducing the importance of the wave loads for bottom-fixed OWTs. One solution is to utilize substructures that are more hydrodynamically transparent. However, the complexity of these structures will lead to increased design and constructions costs. An alternative approach is to utilize the blade pitch and generator control systems to perform active load mitigation (ALM) to counteract the wave loads. This will allow for further expanding the use of monopile foundations.

Numerous researchers have investigated control strategies suitable for performing active load mitigation over the last decades. With focus on reducing the fatigue loading on the support structure, it is demonstrated how the use of the blade pitch control system can increase the aerodynamic damping in operational conditions, leading to reduced response amplitudes in-line with the wind [2–6]. This control strategy will be denoted active aerodynamic damping (AAD) in the following. Furthermore,

*Address all correspondence to this author.

control strategies such as soft cut-out [2,7] and active idling [2,6] may serve to increase the aerodynamic damping in idling conditions. If the cross-wind response is dominating, e.g. due to wind and wave misalignment, it may be beneficial to use active control of the generator torque in order to increase the cross-wind damping [8, 9]. Individual pitch control may also be imposed to provide aerodynamic damping in the cross-wind direction [2, 6, 8].

The efficiency of load mitigation strategies from a design perspective has also previously been investigated. In [2], it was shown how integrating ALM in the design process may result in a significant reduction in steel usage on the support structure of an OWT mounted on a monopile foundation. More recently, it was shown how active use of the control system can allow for using standardized designs over a larger range of site conditions, allowing for reduced design and construction costs [10]. This work also investigated the negative effects of ALM in terms of increased utilization of other wind turbine sub-systems. It was found that use of ALM is most efficient for high wind speeds, while the undesired side effects are most dominant at low wind speeds.

An alternative approach for utilizing active load mitigation will be investigated in this paper. This is motivated by the large contribution to the fatigue damage from unavailability conditions. In these conditions, the lack of aerodynamic damping from the rotor can lead to large response amplitudes. A turbine with reduced availability will therefore experience increased fatigue damage, compared to a turbine with higher availability. To ensure sufficient fatigue capacity, design codes such as [11] require a design availability of no more than 90 %. In [12], the typical contractual availability for an offshore wind farm is cited to be 95 %. Therefore, most turbines in a park will have an unused fatigue capacity exceeding the rules' design fatigue factor at the end of the design lifetime.

The main scientific contribution of this paper is an investigation of the potential for reducing the design fatigue capacity by applying ALM only in turbines experiencing prolonged periods of unavailability. For these turbines, the enlarged fatigue utilization from unavailability conditions can be countered by reducing the fatigue utilization in operational conditions. This will reduce the total design fatigue damage so it is closer to the expected value, while still adhering to the design availability required by the rules. As ALM can lead to adverse side effects in other turbine components, it is desired to limit the use of these control strategies. While ALM can be used in all turbines, this approach will limit the use to turbines experiencing reduced availability. This will allow reducing the design fatigue damage in all turbines while isolating the side effects of ALM to only a few turbines.

The paper is organized as follows: First, the availability characteristics of OWTs are described, before the relevant load mitigation strategies and effects of these are presented. Following this, the simulation setup is given before the results are presented. This will investigate the influence of unavailability on the fatigue damage, the potential of using ALM to counter unavailability effects and the cost of using ALM. The influence of not knowing the true availability of a turbine is also investigated. Finally, the results are discussed and the paper is concluded.

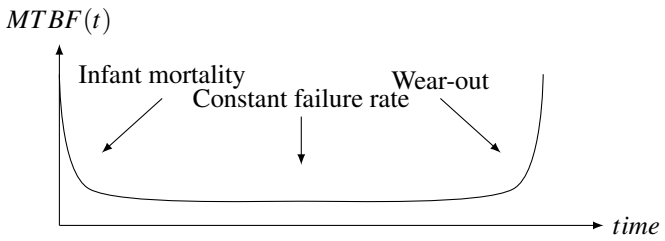

FIGURE 1. VARIATION OF MTBF OVER THE LIFETIME OF A TURBINE

AVAILABILITY OF OWTS

Several factors contribute to the availability of an OWT. Using common engineering models, unavailability may be described by the mean time between failure (MTBF) and the time to repair. Both parameters vary between the different subsystems in the turbine. Further, MTBF is normally time-dependent with higher failure rates occurring in the initial operational phase ("infant mortality") and towards the end of the design life ("wear-out"). In the intermediate stage of a system's life, the failure rate is approximately constant. This behaviour is frequently referred to as the bathtub curve [13, 14], which is illustrated in Fig. 1.

For OWTs, there is limited data concerning availability open to the public. This is mainly caused by the limited number of turbines installed and the fact that many turbines are still in their early years. An analysis of performance data from up to 7000 land-based Danish and German turbines was performed in [13]. This confirmed the occurrence of infant mortality, with a gradually reducing failure rates over time.

A study on failure rates of OWTs has been performed in [14]. This work includes data from approximately 350 turbines in the first eight years of operation, with the majority of the turbines being less than five years old. The overall failure rates do not show a clear trend of following the bathtub curve. Further analyses revealed that only sub-assemblies with infrequent failures seem to follow the bathtub curve [14]. From the data presented, it may also appear as if failures with long repair times follow the bathtub curve, while failures with shorter repair times do not.

While the total failure characteristics of OWTs do not appear to follow the bathtub curve, this paper will investigate means for reducing the effect of infrequent failures leading to prolonged periods of unavailability. For these failures, the results in [14] indicate that the bathtub curve can be an appropriate model.

The above discussion has focused on failure rates. However,

availability is also influenced by the repair time. This depends both on the time spent performing the repairs, and the waiting time before the repair is started. The latter is significantly different for onshore and offshore turbines. For offshore turbines, both the time spent bringing personnel and equipment to the turbine and the time spent waiting for suitable weather conditions may contribute significantly to the total repair time.

LOAD MITIGATION STRATEGIES

While several control strategies are available for reducing the support structure fatigue damage, AAD has been identified as the strategy providing the largest reduction potential [10]. This control method will therefore be utilized in this paper. As the name suggests, active aerodynamic damping reduces the response amplitude of the wind turbine by generating additional aerodynamic forces in phase with the tower top velocity. This is obtained by collective pitching of the blades to generate additional thrust when the rotor nacelle assembly (RNA) is moving into the wind. Similarly, the blade pitch is altered to reduce the aerodynamic thrust when the RNA is moving downwind. As the method provides additional damping, it is well suited for applications on monopile foundations. These are susceptible to significantly dynamical amplification of responses caused by wave loads.

However, AAD is not without negative effects. As shown in [10], there may be a significant increase in both the damage equivalent load and travelled distance of the pitch actuators. Some negative effects can also be experienced in the shaft. As the negative effects are more severe in some environmental conditions, a trade-off must be made. It has been shown that AAD is most effective for high wind speeds, but has low effect for wind speeds below rated [10]. The adverse side effects in the pitch actuators were found to follow the opposite trend. For wind speeds below rated, a significant increase in the use of the pitch actuators was found when AAD was used. At above-rated wind speeds, the penalty on the pitch actuators was less severe. To achieve the desired load reduction in the support structure, it was recommended to activate AAD for wind speeds above a threshold value. The actual value of the threshold will depend on the amount of load reduction required [10].

SIMULATION SETUP

This section will present the simulation model and environmental conditions utilized in the analyses, as well as the criterion used to evaluate the effect of ALM.

Simulation Model

The simulation model is based on the 10 MW reference wind turbine from DTU [15]. Following [16], the tower is stiffened by increasing the wall thickness by 20 % and the inner blade foils are modified. The turbine is placed on a monopile foundation with outer diameter 8.5 metres and a wall thickness of 9 cm. Corresponding to conditions found in the Dogger Bank area, a water depth of 30 m is assumed, while the monopile penetrates 42 metres below the mudline. Furthermore, the turbine is fitted with two tuned mass dampers in the nacelle, mounted perpendicular to each other.

The aero-hydro-servo-elastic simulation tool SIMA from SINTEF Ocean is used to model the turbine. Soil stiffness is modelled using non-linear springs based on p-y curves, calculated in accordance with [17] using soil data from Dogger Bank. Wave kinematics are calculated using linear wave theory and the JONSWAP wave spectrum, while hydrodynamic loads are modelled using MacCamy and Fuchs' load model combined with quadratic Morison-type drag loads. Aerodynamic loads are based on the blade element momentum theory, with corrections for dynamic inflow, dynamic stall, tip loss and tower shadow effects. The wind kinematics are calculated in Turbsim from NREL, using the Kaimal wind spectrum and turbulence class B, as defined in [18]. The structure is modelled using non-linear beam elements, and structural damping is applied as stiffness proportional Rayleigh damping. To account for soil damping the damping coefficient below mudline is double of that above the mudline. Following [19] a total damping level of 1.1 % of critical is assumed for the 1st fore-aft mode when the combined soil and structural damping is taken into account. The total damping level including the tuned mass dampers is 2.1 %, following estimates given in [20].

Operational Modes of Turbine

While most events throughout the lifetime of an OWT will contribute to the total fatigue utilization, only the conditions relevant for unavailability situations and normal turbine operations are considered here. With reference to DNV GL's design standard [11], this corresponds to DLC 1.2, 6.4 and 7.2. These are the power production, idling with wind speeds below cut-in or above cut-out, and idling with fault conditions, respectively. The effects of start-up, shut-down with or without fault and installation are not included.

Modelling of Unavailability To make the unavailability modelling less dependent on site location and turbine type, a detailed modelling of the unavailability is not performed. Rather, the unavailability is applied deterministically and is assumed equally distributed over all environmental conditions.

Furthermore, the additional loading of wind turbine components when active load mitigation is performed may increase the occurrence of faults. This effect has been neglected.

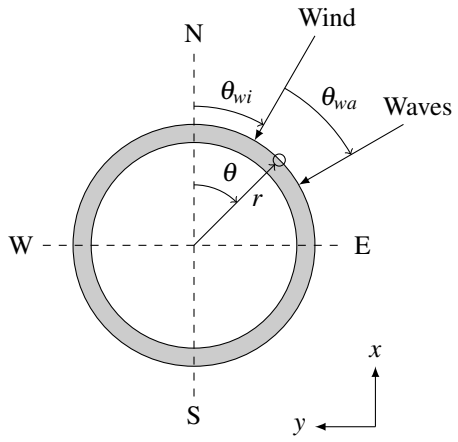

FIGURE 2. COORDINATE SYSTEM OF TURBINE AND ENVIRONMENTAL LOADS.

Environmental Conditions

The environmental conditions simulated are based on 60 years of hindcast data from the Dogger Bank area [21], with statistical properties as described in [22]. Average wind speed, wind direction, significant wave height, wave peak period and wave direction are all available with a temporal resolution of 3 hours. While in principle a five-dimensional joint probability distribution should be used for the simulations, some simplifications have been made. The mean wind direction is considered dependent only on the wind speed, and is binned into bins of 30 degrees. Furthermore, the wave directionality is modelled considering the wind-wave misalignment only, confer Fig. 2. This parameter is also assumed dependent on the wind speed only.

Based on wind speed bins of 1 m/s and wind/wave misalignment bins of 30 degrees an equivalent sea state is generated for each bin from the conditional scatter diagram of H_s and T_p. This is done based on the method described in [23], where the fatigue damage from each environmental condition is approximated by the damage from wind-only and wave-only analyses. This allows for estimating the expected damage from all sea states in a wind speed and misalignment bin. An equivalent sea state giving the same expected fatigue damage can then be found. For the wave-only simulations, the aerodynamic damping of each wind speed bin is accounted for, but wind-wave misalignment is not considered in the wave-only analyses. The resulting load cases are then analysed using 1-hour fully integrated time-domain analyses, with five seeds for each environmental condition.

To further reduce the simulation effort, load cases with a probability of occurrence less than 1/50 of the most probable environmental condition are disregarded. This allows for a significant reduction in the number of load cases to consider, while still accounting for more than 99 % of the environmental conditions. The resulting simulation load cases can be seen in Tab. 2 and Tab. 3.

TABLE 1. PARAMETERS FOR EVALUATION OF EFFECT OF ACTIVE LOAD MITIGATION STRATEGIES.

Component	Parameter	Symbol
Support structure	Max lifetime damage	D
Pitch mechanism	Bearing DEL	DEL_{β}
Pitch mechanism	Actuator usage	ADC
Shaft	Shaft DEL	DEL_{Shaft}

Evaluation of Load Mitigation Effects

While the load mitigation strategies are imposed to reduce the fatigue damage in the support structure, undesirable side effects may occur in other components. Therefore, several parameters will be used for evaluating the effects of ALM. These are summarized in Tab. 1, and will be further detailed in the following sections.

Support Structure Fatigue Evaluation of the fatigue damage in the support structure is performed based on the simulated time series of axial stress. For a position (r,θ) on the cross-section (confer Fig. 2), the axial stress is calculated from the axial force and bending moments using beam theory [24]. Knowing the stress time series the Rainflow counting algorithm implemented in the WAFO toolbox [25] is used to calculate the fatigue utilization, with a correction to account for the 2-slope SN-curve of steel. The appropriate SN-curve for the monopile is assumed to be curve D for steel in seawater with cathodic protection, as given in [26]. For the tower, curve D for steel in air is used. Stress concentration factors due to e.g. welds are disregarded.

Utilization of Wind Turbine Components While active load mitigation strategies are effective for reducing the support structure load levels, they will also influence the utilization of other components in the turbine. In [10], the use of active aerodynamic damping was found to have a positive influence on the blade root damage equivalent loads (DELs). Negligible unfavourable effects were seen in the gearbox DEL, while more severe increases were found in the utilization of the pitch mechanism and the low-speed shaft. The cost of utilizing ALM will therefore be evaluated only for the pitch mechanism and shaft.

For the pitch mechanism, both the loading of the pitch bearings and the use of the pitch actuators may be of concern. Ac-

cording to [27, 28], a rough estimate of the damage equivalent load in the pitch bearings can be calculated as

$$DEL_{\beta} \propto \left(\int |M_o(t)|^m |\dot{\beta}(t)| dt \right)^{1/m} \quad (1)$$

where $M_0(t)$ is the time series of the overturning moment in the bearings, and $\dot{\beta}(t)$ is the rate of change in the pitch angle. The fatigue exponent m depends on the type of bearing used and is here assumed to be 3. This corresponds to a ball bearing [27].

In order to evaluate the increased use of the pitch actuators, the actuator duty cycle (ADC) will be calculated. Following the definition in [29], it can be shown that the ADC is proportional to

$$ADC \propto \int |\dot{\beta}(t)| dt \quad (2)$$

The shaft DEL is estimated based on the torsion moment transferred from the low-speed shaft to the gearbox. This is calculated as

$$DEL_{Shaft} \propto \left(\sum_i^n Q_{shaft,i}^m n_i \right)^{1/m} \quad (3)$$

where n_i is the number of load cycles in the range $Q_{shaft,i}$ of the shaft moment. Further, m is the fatigue exponent, assumed equal to 3 as suggested in [30]. The time series Q_{shaft} is calculated using the following estimate, as described in [31]:

$$Q_{Shaft} = Q_A - (I_R + N_G^2 I_G)\dot{\omega}_R \quad (4)$$

Here, Q_A is the aerodynamic torque, while I_R and I_G are the rotor and generator mass moments of inertia, respectively. N_G is the gear ratio, and $\dot{\omega}_R$ is the angular acceleration of the rotor.

SIMULATION RESULTS

In the following sections, the simulation results are presented. First, the critical position on the monopile is identified. The influence of unavailability is then investigated before the potential for using ALM is explored. The baseline case for results comparison is defined as the traditional design approach: A turbine designed for 90 % availability without the use of ALM.

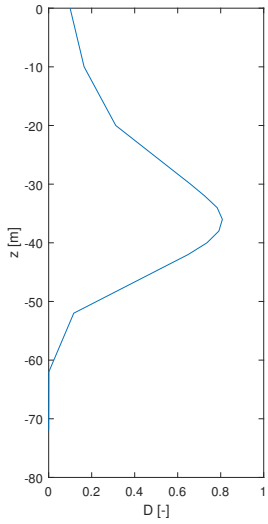

FIGURE 3. DISTRIBUTION OF FATIGUE DAMAGE FROM SEA SURFACE TO BOTTOM OF MONOPILE. Z = -30 M REPRESENTS THE MUDLINE.

Design Fatigue Damage

To identify the most critical position for fatigue damage in the support structure, a fatigue analysis assuming 90 % availability was performed. For the monopile, the resulting fatigue damage is shown in Fig. 3. The most critical location is found to be approximately 8 metres below mudline. All further results for the monopile structure will refer to this position. For the tower, the most critical position is at the tower base.

Fatigue Contributions

Following identification of the most critical cross-section, the important contributions to the fatigue damage in the support structure were analysed. Since no fault is assumed in DLC 1.2 and 6.4, these are considered as availability conditions in the following. DLC 7.2 is considered the only unavailability condition. In Fig. 4, the fatigue damage contribution from availability and unavailability conditions are shown for the critical cross-section on the monopile. It is seen that unavailability conditions contribute with 30 % of the total fatigue damage for a design case with an assumed availability of 90 %. If the availability is increased to 95 %, the unavailability conditions contribute with 17 % of the total fatigue damage. Increasing the availability will also lead to an 11 % reduction in the total fatigue damage.

In Fig. 5, the fatigue damage for different turbine availabilities is compared to the baseline case for the monopile and tower. It is seen that the fatigue damage decreases linearly with increasing availability. The largest reduction seen is 22 % for the

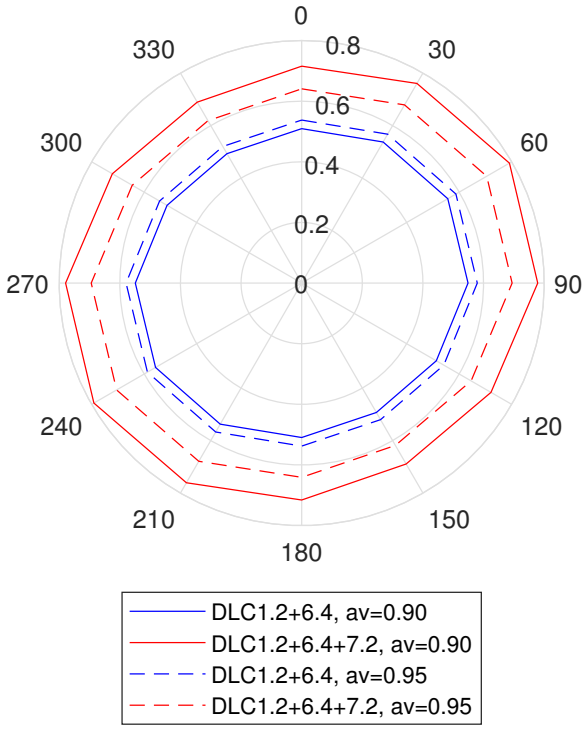

FIGURE 4. CONTRIBUTIONS TO FATIGUE DAMAGE FROM AVAILABILITY (DLC1.2+6.4) AND UNAVAILABILITY (DLC7.2) CONDITIONS. RESULTS ARE PLOTTED FOR AVAILABILITY OF 90 AND 95 %.

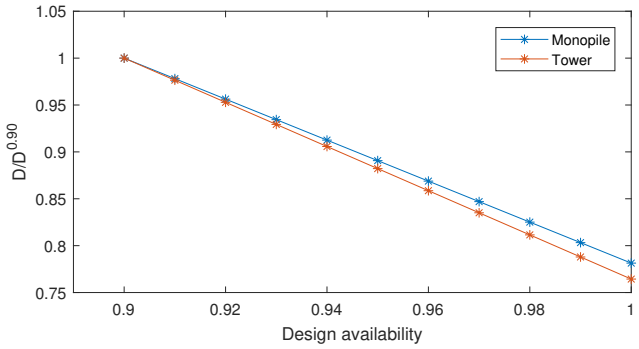

FIGURE 5. MAXIMAL DAMAGE IN THE MONOPILE AND TOWER COMPARED TO DAMAGE FOR 90 % AVAILABILITY AS FUNCTION OF DESIGN AVAILABILITY.

monopile, which is for a turbine with no unavailability. For the tower, the reduction is 24 %. This corresponds to the upper limits of the damage reduction that can be achieved if AAD is used to reduce the effect of unavailability.

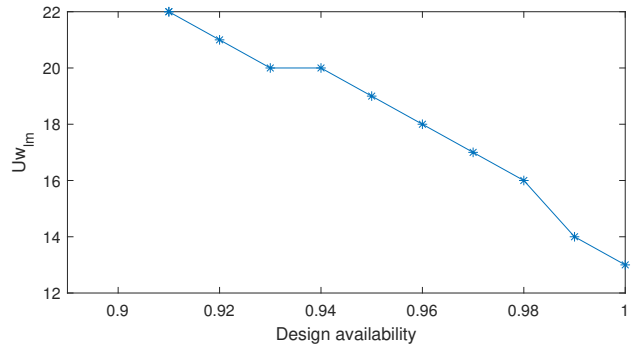

FIGURE 6. WIND SPEEDS FOR ACTIVATION OF AAD TO REDUCE THE FATIGUE DAMAGE TO THE DESIGN VALUE FOR A TURBINE WITH 90 % AVAILABILITY. AAD IS ACTIVATED ABOVE Uw_{lm}.

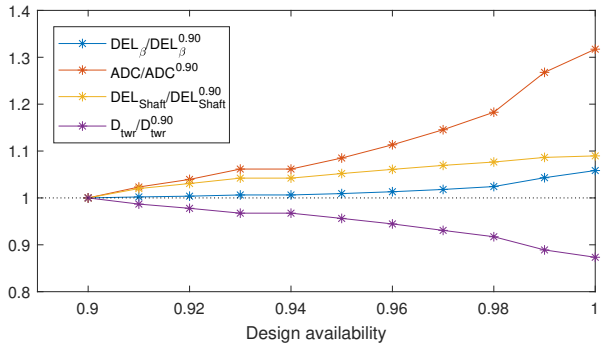

FIGURE 7. VARIATIONS IN COMPONENT UTILIZATION WHEN APPLYING AAD TO REDUCE THE FATIGUE DAMAGE FOR A TURBINE WITH 90 % AVAILABILITY TO THE DAMAGE OBTAINED BY A LARGER DESIGN AVAILABILITY.

Cost of Load Mitigation

In this section, the negative effects of using AAD are analysed using the performance parameters given in Tab. 1. In the analyses, the design fatigue damage corresponding to different availabilities without active load mitigation is calculated for the monopile. Assuming the turbine's true availability is 90 %, active load mitigation is applied to reduce the fatigue damage to the design value. It is assumed that the true availability is known during the full lifetime of the turbine. This corresponds to failures occurring due to infant mortality and expected failure rates through the remaining lifetime, with no wear out of components. AAD is applied at the wind speeds above the limits given in Fig. 6. As an example, a design availability of 95 % will require AAD to be activated for wind speeds above 19 m/s if the true availability is 90 %.

The results are shown in Fig. 7. The abscissa axis shows the availability the turbine is assumed designed for without the use of ALM. On the ordinate axis, the performance parameters are given as values normalized by the performance parameters of a turbine with 90 % availability and no ALM. As expected, the utilization of the components increases with increasing expected availability. This is caused by the reduced design fatigue damage, leading to an increased usage of AAD when the true availability is 90 %.

Furthermore, it can be seen that the cost of AAD increases exponentially for the pitch mechanisms, while the trend is more linear for the shaft DEL. The increase in the pitch mechanism utilization is caused by the excessive pitch activity when AAD is activated at lower wind speeds. This demonstrates the need for a trade-off between fatigue reduction in the support structure and the utilization of other systems.

Figure 7 also shows the reduction in fatigue damage in the tower. This reduction is smaller than the design fatigue reduction in the monopile, which shows that AAD is more effective for the monopile. The analysis above could also be performed using the fatigue damage in the tower as the governing parameter. This would then require a more active use of ALM and a further increased utilization of the pitch mechanism and shaft.

Lack of Knowledge

While the previous analyses have assumed the true availability of the turbine being known during the full lifetime of the turbine, this is an assumption that will not hold in reality. In this section, an analysis will be performed to investigate the effect of this lack of knowledge.

This will be done by assuming the turbine initially operates without the use of ALM. At a predefined time, T_{ALM}, it is assumed that the true availability of the turbine will be known. For the remaining part of the lifetime, the turbine operates with ALM to reach the design fatigue damage in the monopile. This will require a more aggressive use of load mitigation than if the true availability is known before the turbine starts operating. The mode of operation is illustrated in Fig. 8.

As the design standards state that the turbine must be able to withstand 90 % availability, the analysis was performed with this as the true availability. Further, expected availabilities in the range 91-99 % were analysed. The results are shown in Fig. 9, illustrated by the wind speeds for which ALM is used above, Uw_{ALM}. This clearly shows the limitations of using ALM to counter unavailability. If the expected availability is 99 %, load mitigation must be activated during the first 7 years of operation. This will limit the fatigue damage to the design value if the actual availability is 90 %. With an expected availability of 91 %, load mitigation need not be activated within the first 18.5 years of operation. However, Fig. 5 shows that this will only allow for reducing the designed fatigue capacity by 2.2 %.

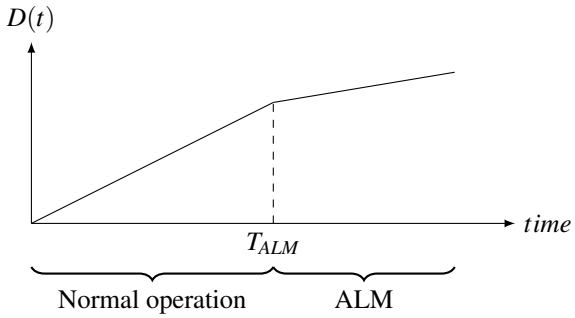

FIGURE 8. OPERATION OF TURBINE WITH ALM UTILIZED AFTER TIME T_{ALM}.

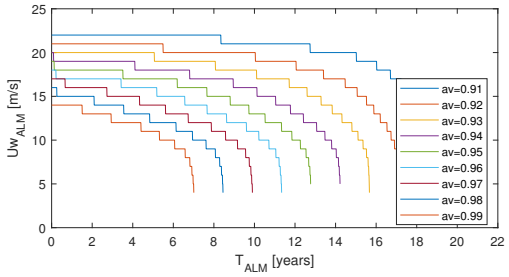

FIGURE 9. WIND SPEED LIMIT FOR ACTIVATION OF AAD AS FUNCTION OF ACTIVATION TIME (T_{ALM}) AND EXPECTED AVAILABILITY (av).

The cost of starting to utilize ALM at different time instances is illustrated for the ADC in Fig. 10. This shows how the utilization of the pitch actuators increases with increasing expected availability. It can also be seen that it is beneficial to start the use of ALM as early as possible. This is due to the fact that late activation of ALM requires the use of load mitigation at lower wind speeds, where the associated cost is significantly higher.

DISCUSSION

The above results demonstrate the abilities and limitations of active load mitigation in reducing the effect of unavailability on the fatigue damage in the support structure. It is clear that it is effective for faults caused by infant mortality. When faults occur close to the end of the intended design life there is not enough time left to counter the increased fatigue damage by ALM.

For the proposed method to be of any use, it is a prerequisite that faults leading to large periods of unavailability occur during the first years of operation. These faults must also be rare events, giving a difference between the expected availability and the true availability. If this difference does not exist, applying ALM on

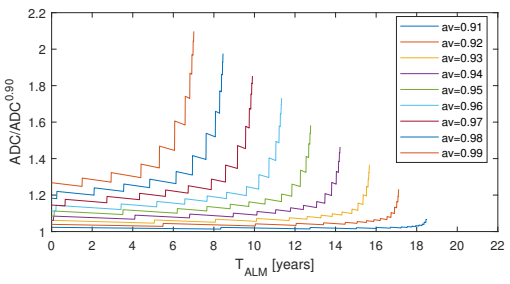

FIGURE 10. INCREASE IN PITCH ADC AS FUNCTION OF FUNCTION OF ACTIVATION TIME FOR AAD (T_{ALM}) AND EXPECTED AVAILABILITY (av).

all turbines may be a more effective approach.

As faults, and thereby availability levels, are inherently random, the actual benefit of using ALM in the proposed way cannot be deduced from the work presented here. It only demonstrates the potential of the method. To assess the actual gain, a structural reliability approach must be taken. In order to obtain realistic results, the availability model must be sufficiently accurate to capture time-dependent variations in the failure characteristics. For the approach to be of practical use, it is a requirement that the model can be established during the design of an OWT so that the reduced fatigue damage may be taken into account by the designer.

CONCLUSION

This paper has investigated the potential of using active load mitigation to counter the negative effects of excessive unavailability in monopile offshore wind turbines. Unavailability conditions contribute with a large share of the support structure fatigue damage. In the analysed 10 MW turbine, 10 % unavailability corresponds to 30 % of the damage.

Design standards require turbines being designed for no more than 90 % availability. The proposed concept is to design the support structure for an availability closer to the expected value. On turbines with lower availability, ALM can be used to counter its effect on the fatigue damage. It is shown that ALM can provide a sufficient load reduction. However, ALM can only realistically be used to counter the effect of faults occurring in the first operational years of the turbine.

ACKNOWLEDGMENT

This work has been carried out at the Centre for Autonomous Marine Operations and Systems (AMOS). The Norwegian Research Council is acknowledged as the main sponsor of NTNU AMOS. This work was supported by the Research Council of Norway through the Centres of Excellence funding scheme, Project number 223254 - AMOS.

REFERENCES

[1] WindEurope, 2018. Offshore Wind in Europe. Key trends and statistics 2017. Tech. rep., WindEurope, Brussels, February.

[2] Fischer, T. A., 2012. "Mitigation of Aerodynamic and Hydrodynamic Induced Loads og Offshore Wind Turbines". PhD Thesis, University of Stuttgart, Stuttgart, July.

[3] van der Hooft, E. L., Schaak, P., and van Engelen, T. G., 2003. Wind turbine control algorithms. Report ECN-C–03-111, ECN, Petten, December.

[4] Bossanyi, E. A., 2003. "Wind Turbine Control for Load Reduction". *Wind Energy,* ***6***(3), June, pp. 229–244.

[5] Bossanyi, E. A., Ramtharan, G., and Savini, B., 2009. "The Importance of Control in Wind Turbine Design and Loading". In 17th Mediterranean Conference on Control and Automation, 2009. MED '09., Mediterranean Control Association, pp. 1269–1274.

[6] Fischer, B., and Shan, M., 2013. A survey on control methods for the mitigation of tower loads. Report 01/104256, Fraunhofer IWES, Kassel, September.

[7] Markou, H., and Larsen, T. J., 2009. "Control strategies for operation of pitch regulated turbines above cut-out wind speeds". In 2009 European Wind Energy Conference and Exhibition, EWEA.

[8] Fischer, T., Rainey, P., Bossanyi, E., and Kühn, M., 2011. "Study on Control Concepts Suitable for Mitigation of Loads from Misaligned Wind and Waves on Offshore Wind Turbines Supported on Monopiles". *Wind Engineering,* ***35***(5), October, pp. 561–573.

[9] Zhang, Z., Nielsen, S., Blaabjerg, F., and Zhou, D., 2014. "Dynamics and Control of Lateral Tower Vibrations in Offshore Wind Turbines by Means of Active Generator Torque". *Energies,* ***7***(11), November, pp. 7746–7772.

[10] Smilden, E., Bachynski, E. E., Sørensen, A. J., and Amdahl, J., 2018. "Site-Specific Controller Design for Monopile Offshore Wind Turbines". *Accepted to Marin Structures*, March.

[11] DNV GL, 2016. DNVGL-ST-0437 Loads and site conditions for wind turbines. Standard, DNV GL, Høvik, November.

[12] Carroll, J., McDonald, A., Dinwoodie, I., McMillan, D., Revie, M., and Lazakis, I., 2017. "Availability, operation and maintenance costs of offshore wind turbines with different drive train configurations". *Wind Energy,* ***20***(2), February, pp. 361–378.

[13] Tavner, P., Xiang, J., and Spinato, F., 2007. "Reliability analysis for wind turbines". *Wind Energy,* ***10***(1), July, pp. 1–18.

[14] Carroll, J., McDonald, A., and McMillan, D., 2016. "Fail-

ure rate, repair time and unscheduled O&M cost analysis of offshore wind turbines". *Wind Energy,* ***19***(6), August, pp. 1107–1119.

[15] Bak, C., Zahle, F., Bitsche, R., Kim, T., Yde, A., Henriksen, L. C., Natarajan, A., and Hansen, M. H., 2013. Description of the DTU 10 MW Reference Wind Turbine. Tech. Rep. 1, DTU Wind Energy, Roskilde, July.

[16] Bachynski, E. E., and Ormberg, H., 2015. "Hydrodynamic modeling of large-diameter bottom-fixed offshore wind turbines". In ASME 2015 34th International Conference on Ocean, Offshore and Arctic Engineering, Vol. **9**, ASME.

[17] The International Organization for Standardization, 2016. ISO 19901-4 Geotechnical and foundation design considerations. Standard, The International Organization for Standardization, Geneva, July.

[18] International Electrotechnical Commision, 2009. Wind turbines - Part 3: Design requirements for offshore wind turbines. Standard, International Electrotechnical Commision.

[19] Suja-Thauvin, L., Krokstad, J. R., and Frimann-Dahl, J. F., 2016. "Maximum Loads on a One Degree of Freedom Model-scale Offshore Wind Turbine". *Energy Procedia,* ***94***, pp. 329–338.

[20] Damgaard, M., Ibsen, L. B., Andersen, L. V., and Andersen, J. K. F., 2013. "Cross-wind modal properties of offshore wind turbines identified by full scale testing". *Journal of Wind Engineering and Industrial Aerodynamics,* ***116***, pp. 94–108.

[21] Reistad, M., Breivik, y., Haakenstad, H., Aarnes, O. J., Furevik, B. R., and Bidlot, J., 2011. "A high-resolution hindcast of wind and waves for the North Sea, the Norwegian Sea, and the Barents Sea". *Journal of Geophysical Research: Oceans,* ***116***(C5), May.

[22] Horn, J.-T. H., Krokstad, J. R., and Amdahl, J., 2017. "Joint probability distribution of environmental conditions for design of offshore wind turbines". In ASME 2017 36th International Conference on Ocean, Offshore and Arctic Engineering, Vol. **1**, ASME.

[23] Kühn, M. J., 2001. "Dynamics and design optimisation of offshore wind energy conversion systems". PhD Thesis, TU Delft, Delft University of Technology, Delft, June.

[24] Kvittem, M. I., and Moan, T., 2015. "Time domain analysis procedures for fatigue assessment of a semi-submersible wind turbine". *Marine Structures,* ***40***, November, pp. 38–59.

[25] WAFO-group, 2017. *WAFO - A Matlab Toolbox for Analysis of Random Waves and Loads - A Tutorial*. Math. Stat., Center for Math. Sci., Lund Univ., Lund, Sweden. See also URL `http://www.maths.lth.se/matstat/wafo`.

[26] DNV GL, 2016. DNVGL-RP-C203 Fatigue design of offshore steel structures. Standard, DNV GL, Høvik, April.

[27] Burton, T., Jenkins, N., Sharpe, D., and Bossanyi, E., 2011. *Wind Energy Handbook*. Wiley, Hoboken.

[28] Shan, M., Jacobsen, J., and Adelt, S., 2013. "Field Testing and Practical Aspects of Load Reducing Pitch Control Systems for a 5 MW Offshore Wind Turbine". In European Wind Energy Conference and Exhibition (EWEC), EWEA.

[29] Bottasso, C. L., Campagnolo, F., Croce, A., and Tibaldi, C., 2013. "Optimization-based study of bend-twist coupled rotor blades for passive and integrated passive/active load alleviation". *Wind Energy,* ***16***(8), November, pp. 1149–1166.

[30] Stol, K. A., Zhao, W., and Wright, A. D., 2006. "Individual Blade Pitch Control for the Controls Advanced Research Turbine (CART)". *Journal of Solar Energy Engineering,* ***128***(4), November, pp. 498–505.

[31] Nejad, A. R., Gao, Z., and Moan, T., 2014. "On long-term fatigue damage and reliability analysis of gears under wind loads in offshore wind turbine drivetrains". *International Journal of Fatigue,* ***61***, November, pp. 116–128.

Appendix A: Environmental Load Cases

TABLE 2. Environmental parameters for lowest wind speeds. Light grey cells give H_s in m, grey cells give T_p in s, while dark grey cells give probability of occurrence in %. Wind speeds are given in m/s

Wind Speed	Misalignment angle						
	0°	30°	60°	90°	120°	150°	180°
2.6	1.1	1.2	1.1	1.1	1.1	1.1	1.1
	6.2	6.4	6.4	6.6	6.6	6.6	6.6
	0.79	1.56	1.34	1.56	1.02	0.66	0.53
4	1.1	1.1	1.2	1.1	1.1	1.1	1.0
	6.1	6.3	6.4	6.7	6.7	6.9	6.7
	0.61	1.21	0.96	0.89	0.55	0.33	0.29
5	1.2	1.2	1.2	1.2	1.1	1.1	1.1
	6.0	6.1	6.4	6.7	6.9	6.7	6.9
	0.99	1.73	1.13	0.98	0.56	0.34	0.26
6	1.3	1.3	1.3	1.2	1.1	1.1	1.1
	5.8	6.0	6.5	6.8	7.1	6.9	6.9
	1.47	2.23	1.21	0.98	0.49	0.31	0.24
7	1.3	1.3	1.3	1.3	1.3	1.2	1.2
	5.6	5.9	6.4	6.9	7.1	7.3	7.3
	1.96	2.74	1.16	0.75	0.44	0.24	0.20
8	1.4	1.5	1.5	1.4	1.3	1.4	1.2
	5.5	5.9	6.5	7.1	7.3	7.6	7.5
	2.61	3.09	1.07	0.61	0.31	0.17	0.15
9	1.5	1.6	1.7	1.5	1.4	1.4	1.3
	5.4	5.9	6.9	7.4	7.7	7.6	7.4
	3.20	3.31	0.88	0.46	0.23	0.14	0.10
10	1.6	1.8	1.8	1.8	1.6		
	5.5	6.0	6.8	7.8	7.8		
	3.66	3.19	0.64	0.31	0.13		
11	1.8	1.9	2.0	1.9	1.6		
	5.6	6.1	7.0	8.3	8.2		
	3.97	2.76	0.42	0.18	0.08		
12	2.0	2.2	2.1	2.1			
	5.8	6.3	7.3	8.3			
	3.96	2.30	0.29	0.09			
13	2.2	2.4	2.4				
	6.1	6.5	7.4				
	3.71	1.87	0.17				

TABLE 3. Environmental parameters for highest wind speeds. Light grey cells give H_s in m, grey cells give T_p in s, while dark grey cells give probability of occurrence in %. Wind speeds are given in m/s

Wind Speed	Misalignment angle						
	0°	30°	60°	90°	120°	150°	180°
14	2.5	2.6	2.6				
	6.4	6.8	7.3				
	3.37	1.40	0.10				
15	2.7	2.9					
	6.7	6.9					
	2.99	1.08					
16	3.0	3.1					
	7.0	7.2					
	2.59	0.82					
17	3.3	3.3					
	7.3	7.5					
	2.15	0.57					
18	3.5	3.6					
	7.5	7.7					
	1.74	0.38					
19	3.8	3.8					
	7.9	7.9					
	1.33	0.30					
20	4.1	4.1					
	8.1	8.1					
	1.12	0.21					
21	4.4	4.5					
	8.3	8.4					
	0.77	0.14					
22	4.6	4.7					
	8.4	8.5					
	0.50	0.08					
23	4.9						
	8.6						
	0.34						
24	5.2						
	8.7						
	0.19						
26.3	6.0						
	9.3						
	0.28						